Numerical and experimental investigation of the effect of filtering on chaotic symbolic dynamics

Liqiang Zhu[a)]
Department of Electrical Engineering, Center for Systems Science and Engineering Research, Arizona State University, Tempe, Arizona 85287

Ying-Cheng Lai and Frank C. Hoppensteadt
Department of Electrical Engineering, Center for Systems Science and Engineering Research, Arizona State University, Tempe, Arizona 85287
and Department of Mathematics, Arizona State University, Tempe, Arizona 85287

Erik M. Bollt
Department of Mathematics and Computer Science, Clarkson University, Potsdam, New York 13699

(Received 12 April 2002; accepted 20 September 2002; published 21 February 2003)

Motivated by the practical consideration of the measurement of chaotic signals in experiments or the transmission of these signals through a physical medium, we investigate the effect of filtering on chaotic symbolic dynamics. We focus on the linear, time-invariant filters that are used frequently in many applications, and on the two quantities characterizing chaotic symbolic dynamics: topological entropy and bit-error rate. Theoretical consideration suggests that the topological entropy is invariant under filtering. Since computation of this entropy requires that the generating partition for defining the symbolic dynamics be known, in practical situations the computed entropy may change as a filtering parameter is changed. We find, through numerical computations and experiments with a chaotic electronic circuit, that with reasonable care the computed or measured entropy values can be preserved for a wide range of the filtering parameter. © *2003 American Institute of Physics.* [DOI: 10.1063/1.1520090]

Experimentally measured signals are either inevitably or intentionally filtered, the former can be attributed to the limitation of the measuring instruments while the latter is due to the necessity to remove undesirable frequency components for signal processing. Another area where filtering is relevant is transmission of chaotic signals through a physical medium. For instance, in a communication application, a chaotic wave form is transmitted through a channel. Because of the finite bandwidth of the channel, the transmission is equivalent to a filtering process. Most existing works on the effect of filtering on chaotic signals deal with how filtering changes the fractal dimensions, with well-known results such as the dimension increase caused by filtering. The focus of our investigation is on the symbolic-dynamics aspect of chaotic signals. Suppose a dynamical system generates a chaotic signal with a well-defined symbolic dynamics, and suppose this signal is filtered. We ask, to what extent is the chaotic symbolic dynamics affected by filtering. To be concrete, we focus on the topological entropy and the bit-error rate, two quantities characterizing the symbolic dynamics. Theoretical considerations indicate that the topological entropy is invariant under linear filtering, which we have verified using numerical computations and experiments with a chaotic electronic circuit. Our results suggest that in practical situations, with reasonable care, the estimated topological entropy can be preserved and the bit-error rate can be maintained at low values for a wide range of the filtering parameter.

I. INTRODUCTION

The effect of filtering on chaotic signals has been a topic of interest since the pioneering work of Badii *et al.*,[1] who observed that linear, infinite-impulse response (IIR) filters tend to increase the fractal dimension of the attractor reconstructed from a filtered chaotic signal. In particular, let $d\mathbf{x}/dt=\mathbf{F}(\mathbf{x})$ be the original dynamical system generating a chaotic attractor, where $\mathbf{x}\in\mathcal{R}^N$, and let $x(t)$ be one of the components of $\mathbf{x}$ which is to be filtered. The simplest, first-order IIR filter may be represented by the following linear differential equation:

$$\frac{dz}{dt}=-\eta z+x(t), \tag{1}$$

where $z(t)$ is the filtered signal and $0<\eta<1$ is the filtering parameter. For such a filter, if an attractor is reconstructed from the filtered signal $z(t)$, the fractal dimension of the attractor can be higher than that of the original attractor.[1,2]

The argument for the dimension increase goes as follows.[1,2] Consider the Kaplan–Yorke formula[3] for the Lyapunov dimension,

$$D_L=k+\frac{1}{|\lambda_{k+1}|}\sum_{i=1}^{k}\lambda_i,$$

[a)]Electronic mail: lqzhu@asu.edu

which is conjectured to be equal to the information dimension of the attractor, where λ_i's $(i=1,\ldots,N)$ are the Lyapunov exponents and k is the largest integer for which the sum $\Sigma_{i=1}^{k}\lambda_i$ is positive. A linear, time-invariant filter, as represented by Eq. (1), gives an additional Lyapunov exponent $\ln\eta<0$ (for typical cases where $0<\eta<1$). If $\ln\eta$ lies in between λ_{k+1} and λ_k such that $\Sigma_{i=1}^{k}\lambda_i>0$ but $\Sigma_{i=1}^{k}\lambda_i+\ln\eta<0$, a situation that can be expected in low-dimensional chaotic systems, the Lyapunov dimension of the filtered signal is increased to

$$D_L^{\mathrm{fil}}=k+\frac{1}{|\ln\eta|}\sum_{i=1}^{k}\lambda_i>D_L\,.$$

Analysis also indicates that the increase can be due to the fact that a chaotic attractor typically resides on a fractal surface that is continuous but not differentiable.[4,5] The work of Broomhead *et al.* reveals that the time extent of a filter is important and can have nontrivial effects on chaotic signals.[6] Specifically, finite-impulse-response (FIR) filters tend to induce a diffeomorphism between the original and the filtered attractors and, hence, generally they preserve the dimension. An important recent result in this area is the development of statistical measures for testing continuity and differentiability by Pecora and Carroll,[7] which can be powerful for studying the effect of filtering on chaotic signals and other related problems such as generalized synchronization[5,8] as well.

The problem of filtering is important because, in experimental or applied situations, measurements of chaotic signals involve a hierarchy of physical instruments, each affecting the amplitude and frequency characteristics of the signal and, hence, each can be regarded as a filter. Another example is the *in-principle* exploration of the idea of communicating with chaos by utilizing synchronous chaos[9] or chaotic symbolic dynamics.[10–12] In the first approach, a message is mixed with a chaotic signal through a modulation process at the transmitter, and the receiver extracts the message by subtracting off the chaotic signal, provided that a synchronous copy of the signal is available from a replica of the chaotic system that generates the original chaotic signal. In the second approach, a message is encoded into a chaotic signal by making use of the symbolic dynamics of the underlying dynamical invariant set. In both cases, a chaotic wave form carrying information is to be transmitted through a physical channel. The channel is, of course, imperfect and possesses practical limitations ranging from finite bandwidth to dissipation.

A chaotic signal is characterized by a variety of dynamical and topological invariants such as the fractal dimension spectrum, the Lyapunov exponent spectrum, the topological and metric entropies. Most previous works focus on the dimension aspect of the filtering problem. In this paper, we study the effect of filtering on the symbolic dynamics of chaotic signals.[13] In particular, we consider a general dynamical system that involves the original dynamical system $d\mathbf{x}/dt=\mathbf{F}(\mathbf{x})$ and an IIR filter, and ask the following questions: (1) to what extent is the topological entropy h_T of the original chaotic attractor affected by filtering? (2) Suppose a sequence of symbols is embedded in the original chaotic signal $x(t)$, to what degree will the sequence be altered after filtering, i.e., what is the bit-error rate (BER) caused by filtering?

Topological entropy is defined with respect to the symbolic dynamics of the underlying chaotic system. Consider a dynamical system described by $f:M\to M$, which is defined on a compact set M. By partitioning M into a collection of subsets $P=\{P_1,\ldots,P_p\}$, one can obtain a symbolic sequence for a typical trajectory according to its order of visits to these subsets. Let $f^{-k}[P]$ denote the partition $\{f^{-k}(P_1),\ldots,f^{-k}(P_p)\}$ and $P^{(n)}$ be the partition $\{P\cap f^{-1}[P]\cap\cdots\cap f^{-n+1}[P]\}$. The topological entropy of M with respect to partition P is[14]

$$h_T(M,P)=\lim_{n\to\infty}\frac{1}{n}\log N(P,n), \tag{2}$$

where $N(P,n)$ is the smallest number of sets in $P^{(n)}$ that still covers M, or the total number of all possible symbolic sequences with length n. In general, the value of the topological entropy depends on the partition P. To have a unique entropy associated with the symbolic dynamics, one utilizes the *generating partition* P^*[15] that generates a one-to-one correspondence between the phase space and the abstract symbolic space and yields the largest entropy value among those from all possible partitions

$$h_T(M)=\sup_P h_T(M,P)=h_T(M,P^*). \tag{3}$$

In one dimension, the generating partition is the set of critical points of the map. In high dimensions, it is generally difficult to find the generating partition.[16,17] For this reason, in this paper we choose as working examples chaotic systems that are equivalent to one-dimensional maps on a Poincaré surfaces of section.

To argue for the invariance of the topological entropy under filtering, we consider the Kolmogorov–Sinai (KS) entropy $h_{\mathrm{KS}}(\mu)$, which gives the rate of information creation with respect to an ergodic invariant measure μ. The topological entropy can be related to the KS entropy as[18]

$$h_T(M)=\sup_\mu h_{\mathrm{KS}}(\mu). \tag{4}$$

The KS entropy, in turn, can be related to the Lyapunov spectrum associated with the measure μ,

$$h_{\mathrm{KS}}(\mu)\leqslant\Sigma_{\lambda_i>0}\lambda_i\,, \tag{5}$$

where the equality holds for Hamiltonian systems for which the measure of interest is the volume fraction of the relevant chaotic ergodic region,[19] and for Axiom-A systems as well.[18] Since linear filtering does not change the *positive* Lyapunov exponents of the system, Eqs. (4) and (5) imply that both the KS and the topological entropies are invariant under linear filtering.

A complication is that the attractor of the filtered system resides on a compact set M' which in general is different from the compact set M of the original attractor. Because of the change in the geometry and topology of the attractor (as reflected, e.g., by a possible increase in the fractal dimension), the generating partition of the filtered attractor will be

altered. We find, through numerical computations and experimental measurements, that it is usually more difficult to find the generating partition if the degree of filtering is relatively severe. The topological entropy with respect to the generating partition of the unfiltered attractor is thus still of interest. For a given filtering parameter, we will then consider two entropies: $h_T(P^{*0})$ and $h_T(P^*)$, the topological entropies computed with respect to the generating partition of the original, unfiltered attractor and to that of the filtered attractor, respectively. We expect $h_T(P^{*0})$ to decrease as filtering becomes severe but $h_T(P^*)$ to remain invariant, unless in cases where the generating partition of the filtered attractor cannot be found. A similar consideration applies to BER: we expect it to increase under filtering with respect to the fixed partition P^{*0} but to remain low with respect to the generating partition of the filtered attractor. To verify these results, we focus on a typical class of low-pass IIR filters and compute how $h_T(P^{*0})$, $h_T(P^*)$ and BER change as functions of the cutoff frequency of the filter, by using both numerical and actual experiments. In our study, these entropies are estimated directly according to their definitions. Specifically, for $h_T(P^{*0})$, we count $N(P,n)$, the number of distinct symbolic sequences of length n, defined with respect to the fixed partition P^{*0}, for n up to a value determined by the numerical limitation (20 for numerical computations and 13 for experimental data). The slope of the linear fit between $\ln N(P,n)$ and n gives an approximate value of $h_T(P^{*0})$. For $h_T(P^*)$, we perform the same computation but with respect to the generating partition P^*. While there are other methods for computing the topological entropies of one-dimensional maps such as the Markov approach[20] and the kneading-sequence approach,[21] we find that our direct approach is more suitable, particularly for experimental data.

The principal results of this paper are: (1) the topological entropy for chaotic flow is verified to be invariant under linear filtering; (2) in the practical situation, by exercising reasonable care (to be detailed in the following), the estimated topological entropy can be preserved and the bit-error rate can be maintained at low values for a wide range of the filtering parameter. The implication is that measurements of chaotic signals by physical instruments or the transmission of chaotic signals through a physical medium can be regarded as a process that mostly preserves the symbolic representation of the signal.

The rest of the paper is organized as follows. In Sec. II, we present a numerical example with a continuous-time chaotic flow to illustrate the effect of filtering. In Sec. III, we suggest theoretical models to understand the behavior of the topological entropy as a function of the filtering parameter and to explain why the entropy can be preserved in principle. In Sec. IV, we present experimental results from a chaotic electronic circuit with filtering, which are consistent with our numerical and theoretical analysis. In Sec. V, we briefly discuss the relevance of our work to signal processing in a biomedical application.

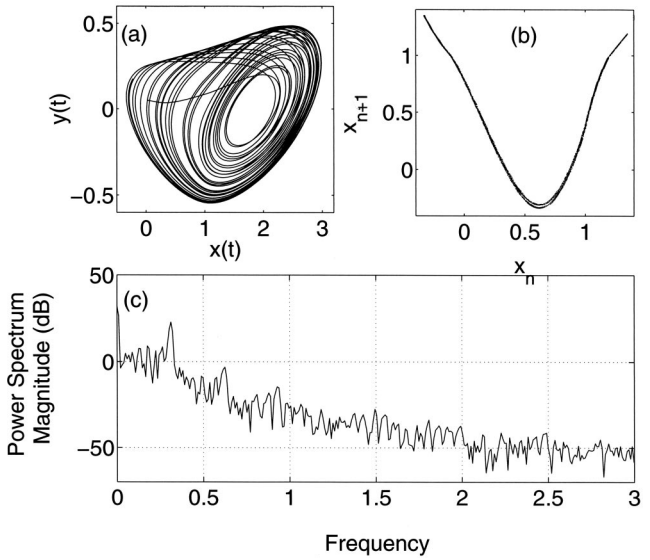

FIG. 1. (a) A single-scroll chaotic attractor from Chua's circuit projected on the (x,y) plane. (b) The return map constructed by recording the local minima x_n of time series $x(t)$. (c) Fourier power spectrum of $x(t)$. The bandwidth of $x(t)$ is about 0.66.

II. A NUMERICAL EXAMPLE

We use Chua's circuit[22] as our paradigmatic numerical and experimental system to investigate the effect of filtering. The differential equations that describe the circuit, in a dimensionless form, are

$$\frac{dx}{dt} = \alpha_1(y-x) - \beta_1 f(x),$$
$$\frac{dy}{dt} = \alpha_2(x-y) + \beta_2 z, \tag{6}$$
$$\frac{dz}{dt} = -\gamma y,$$

where the dynamical variables x, y, and z are proportional to the voltage drops across the two capacitors, and the current through the inductor in the circuit, respectively. The nonlinearity comes from the piecewise linear function: $f(x) = Bx + (A-B)[|x+E| - |x-E|]/2$, where A, B, and E are constants. An advantage of Chua's circuit is that a variety of chaotic behaviors can be generated by changing the circuit parameters. For instance, one can obtain both double-scroll, Lorenz-type[23] and single-scroll, Rössler-type[24] chaotic attractors. To facilitate analysis, in this paper we focus on the single-scroll family, as the corresponding return-maps generally resemble a quadratic map. An example is shown in Fig. 1(a), where the parameters are: $\alpha_1 = 5.94$, $\beta_1 = 9.0$, $\alpha_2 = 0.66$, $\beta_2 = 1.0$, $\gamma = 7.0$, $A = -0.5$, $B = -0.8$, and $E = 1.0$. To obtain a return map, we locate x_n $(n = 0,1,\ldots)$, the successive local minima of the dynamical variable $x(t)$, and plot x_{n+1} vs x_n, as shown in Fig. 1(b). The return map defined by $x_{n+1} = F(x_n)$ is apparently approximately one-dimensional with a quadratic minimum. Figure 1(c) shows the power spectrum of $x(t)$. The bandwidth of the spectrum is about 0.66.

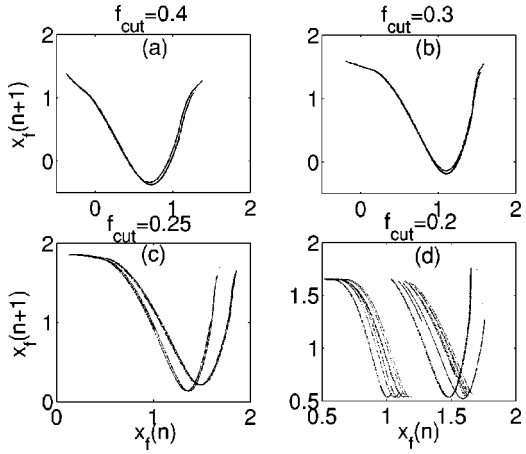

FIG. 2. (a)–(d) Return maps obtained from the filtered signal of $x(t)$ for cutoff frequency $f_{\text{cut}}=0.4$, 0.3, 0.25, and 0.2, respectively.

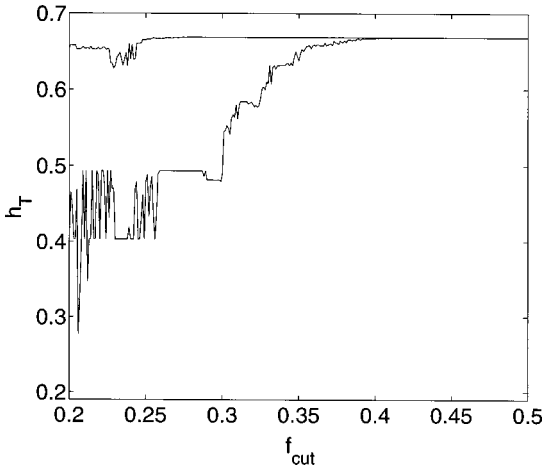

FIG. 3. Computed topological entropy vs cutoff frequency. The lower trace is with respect to the original partition and the upper trace is with respect to the optimal partitions. See the text for details.

In applications, Butterworth filters, which are IIR filters, are most frequently used. An nth-order Butterworth lowpass filter is described by a frequency response function [the Fourier transform of filter's impulse-response function $b(t)$] with magnitude given by[25]

$$|B(\omega)|^2=\frac{1}{1+(\omega/\omega_c)^{2n}}, \tag{7}$$

where ω_c is the cutoff frequency. The corresponding Laplace transform $B(s)$ of $b(t)$ contains n poles, typically chosen to be those in the left-half plane of the complex s-plane. If $u(t)$ and $v(t)$ denote the input and output of the filter, respectively, then in the time domain, the nth order Butterworth lowpass filter is described by the following nth order linear differential equation:

$$\frac{d^n v(t)}{dt^n}+A_{n-1}(\omega_c)\frac{d^{n-1}v(t)}{dt^{n-1}}+\cdots+A_1(\omega_c)\frac{dv(t)}{dt}+\omega_c^n v(t)=\omega_c^n u(t), \tag{8}$$

where the coefficients $A_1(\omega_c),\ldots,A_{n-1}(\omega_c)$ depend on the cutoff frequency.

To numerically investigate the effect of filtering, we utilize a fifth-order Butterworth low-pass filter with cutoff frequency ranging from 0.2 to 0.6 and pass one of the dynamical variables through the filter. In order to mimic an experimental situation, we digitally sample the signal $x(t)$ before filtering at a frequency about 30 times higher than the Nyquist frequency of the signal. Let $x_f(t)$ be the signal after filtering. Figures 2(a)–2(d) show the return maps constructed from $x_f(t)$ for cutoff frequency at $f_{\text{cut}}=0.4$, 0.3, 0.25, and 0.2, respectively. Comparing with the return map from $x(t)$ [before filtering, Fig. 1(b)] which roughly contains one branch and is therefore approximately one-dimensional, we see that severe filtering induces a multibranch structure in the return map, indicating an increase in the fractal dimension of the filtered signal. The smaller the cutoff frequency, the more apparent the high-dimensional structure [Figs. 2(c) and 2(d)]. We also note that, even in the cases of high cutoff frequencies [Figs. 2(a) and 2(b)] where the return maps are still approximately one-dimensional, the locations of the critical point appear to have shifted, as compared with the location of the original map [Fig. 1(b)]. Since the location of the critical point defines the generating partition, the observation is then that, when the degree of filtering is weak, i.e., when the cutoff frequency of the lowpass filter is high, the effect of filtering is simply a shift in the location of the generating partition for defining the symbolic dynamics.

We first examine the topological entropy $h_T(P^{*0})$ as a function of the cutoff frequency of the lowpass filter, where the partition P^{*0} is located at the critical point of the unfiltered return map. If f_{cut} is about the bandwidth Δf of the chaotic signals, the resulting return map remains approximately the same as that from the original signal, in both shape and location. This leads to almost identical values for the topological entropy $h_T(P^{*0})$, as shown in Fig. 3 (the lower trace for $f_{\text{cut}}>0.4$). When f_{cut} is decreased from the value of Δf, the $h_T(P^{*0})$-vs-f_{cut} function appears to exhibit a nonmonotone behavior, as shown in Fig. 3 (the lower trace for $0.28\lesssim f_{\text{cut}}<0.4$). In this range of the cutoff frequency, the return map from the filtered signal is still approximately single-branched. The intriguing behavior in the topological entropy thus comes almost purely from the change in the location of the critical point of the return map.[26,27] If f_{cut} is several times smaller than Δf, then the reconstructed return map will contain multiple branches at various locations, indicating an increase in the underlying dimensionality of the filtered signal $x_f(t)$, which results in the large fluctuations in $h_T(P^{*0})$.

We next study the behavior of $h_T(P^*)$ as a function of f_{cut}, where P^* is the generating partition of the filtered return map, which depends on f_{cut}. If $f_{\text{cut}}<\Delta f$, it is straightforward to find P^* because the filtered return map is still approximately one-dimensional so that its critical point defines P^*. If $f_{\text{cut}}\ll\Delta f$, the filtered return map appears no longer one-dimensional. In this case, identifying the generating partition is difficult.[16,17] We thus use the following simple practical procedure: we place the symbolic partition at a series of systematically chosen locations in the range of the return map, compute the topological entropy for each

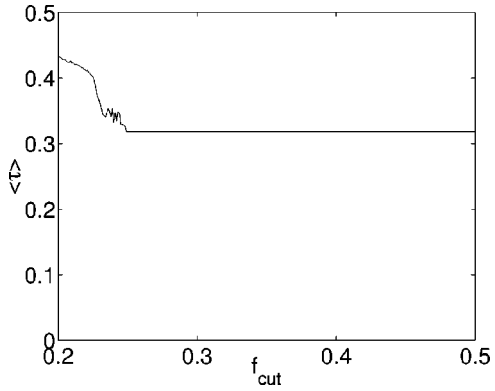

FIG. 4. The average first-return time $\langle \tau \rangle$ vs the cutoff frequency of the lowpass filter.

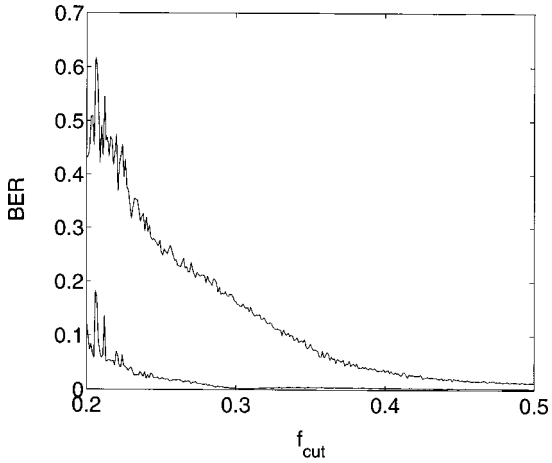

FIG. 5. The bit-error-rate (BER) vs the cutoff frequency of the lowpass filter. The upper trace is with respect to the original partition and the lower trace is with respect to optimal partitions.

location, and determine the one that yields the maximum value of the entropy. Although the partition so chosen is optimal in the sense described (we call it *optimal partition*), it will not be generating, as the true partition can be quite complicated because of the high dimensionality underlying the filtered signal. The resulting entropy function is shown in Fig. 3 (the upper trace). We see that the entropy so obtained has approximately the same value as that from the original, unfiltered system.

The approximately constant behavior of the topological entropy (upper trace in Fig. 3) does not directly support the conjecture that h_T for filtered chaotic flow f is invariant. It only suggests that h_T for a Poincaré map is invariant under filtering. The KS entropy of the flow can be related to that of the Poincaré map by Abramov's formula,[18]

$$h_{\mathrm{KS}}^{\mathrm{flow}} = \frac{h_{\mathrm{KS}}^{\mathrm{map}}}{\langle \tau \rangle}, \tag{9}$$

where τ is the average first-return time. Assuming that a similar relation holds for the topological entropy, we see that the entropy should be invariant under filtering for flow only if $\langle \tau \rangle$ is approximately unchanged under filtering. For our numerical example, the behavior of $\langle \tau \rangle$ vs f_{cut} is shown in Fig. 4. Apparently, $\langle \tau \rangle$ is invariant if $f_{\mathrm{cut}} > 0.25$, where the filtered return map is still approximately one-dimensional [Figs. 2(a)–2(c)]. Figures 3 and 4 suggest that the topological entropy of the flow is invariant if filtering is not severe. For $f_{\mathrm{cut}} < 0.25$, the average first-return time increases as f_{cut} is decreased, indicating that on average, the topological entropy of the flow should be decreased. These considerations are heuristic of course. If there exists a probability measure, with respect to which $\langle \tau \rangle$ remains invariant under filtering, then the topological entropy of the chaotic flow defined with respect to this measure can be invariant under filtering. We are not aware of any procedure for finding such a measure.

While the topological entropy characterizes how ''random'' a chaotic signal is, it does not quantify the ''correctness'' of the transmitted symbolic sequence. In the context of communication where a chaotic system is employed to encode information, this entropy in fact quantifies the ''channel capacity'' of the chaotic system.[10] The appropriate quantity to characterize how correct the symbolic dynamics can be extracted after transmission is BER. If the degree of filtering is severe, we expect a high BER. To compute the BER, we choose a chaotic signal corresponding to an information string of 10^4 symbols, pass the signal through a lowpass filter, and then calculate the fraction of converted symbols (the wrongly extracted ones). If the partition is fixed and chosen as the one from the original, unfiltered chaotic signal, we expect a high value of BER when the cutoff frequency of the filter is such that the return map is either shifted and/or multibranched. However, if we use optimal partitions, we expect to be able to reduce the BER significantly, at least in the range of cutoff frequency where the return maps from the filtered signal remain single-branched. These results are shown in Fig. 5, where the upper trace is BER vs f_{cut} for a fixed partition, and the lower trace is that for optimal partitions. We see that if the cutoff frequency is high ($f_{\mathrm{cut}} > 0.4$), the BER is low. However, for $0.28 \leq f_{\mathrm{cut}} < 0.4$, the BERs are quite high if a fixed partition is chosen but they can be reduced significantly if optimal partitions are chosen for different cutoff frequencies, insofar as the return map remains approximately single-branched. For $f_{\mathrm{cut}} < 0.28$, the BER is appreciable even with the use of optimal partitions. The heuristic reason is, of course, that the return maps are generally multibranched, and the optimal partitions are not even approximations of the corresponding generating partitions, leading to severe confusion in the specification of symbols. Thus, we see that, from the standpoint of delivering information correctly, the cutoff frequency of the lowpass filter should be higher than a critical value, below which the dynamics of the unfiltered and filtered chaotic signals are topologically different. If there is an apparent increase in the dimensionality of the filtered signal, the information carried by the signal can be destroyed by the physical medium through which a chaotic signal is transmitted.

III. HEURISTIC ANALYSIS OF THE ENTROPY FUNCTION

To better understand how linear filtering affects the topology of a chaotic system and to gain intuition about the

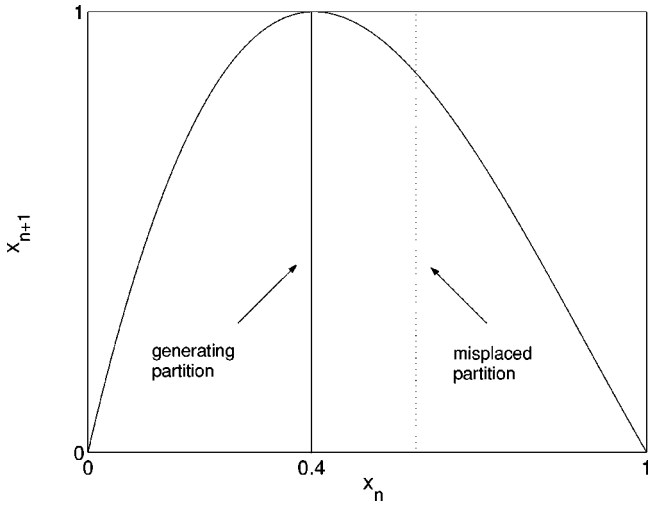

FIG. 6. The skew Ulam map $f(x)=cx(1-x)(1-bx)$, $b=0.6$, $c=17.4$. There is a critical point at $x_c\approx 0.4$.

invariance of the topological entropy under filtering, we consider a simple analyzable model, the one-dimensional Ulam map,[28] which reads

$$x_n=F(x_{n-1})=cx_{n-1}(1-x_{n-1})(1-bx_{n-1}), \tag{10}$$

where b and c are parameters. Choosing $b=0.6$ and $c=17.4$, the critical point of the map is located at $x_c\approx 0.4$ and the map generates a chaotic attractor in the unit interval, as shown in Fig. 6. Consider the following first-order lowpass IIR filter:

$$y_n=\epsilon y_{n-1}+(1-\epsilon)x_n, \tag{11}$$

where $\epsilon\equiv\exp(-\eta)$ and η is the the cutoff frequency of the filter. The new system can be represented by a two-dimensional map,

$$\begin{aligned} x_n&=cx_{n-1}(1-x_{n-1})(1-bx_{n-1}),\\ y_n&=\epsilon y_{n-1}+(1-\epsilon)x_n. \end{aligned} \tag{12}$$

Since x can be considered as a random variable in the unit interval, we obtain

$$\begin{aligned} y_n&=(1-\epsilon)x_n+\epsilon y_{n-1}\\ &=(1-\epsilon)x_n+\epsilon((1-\epsilon)x_{n-1}+\epsilon y_{n-2})\\ &=(1-\epsilon)x_n+\epsilon((1-\epsilon)x_{n-1}\\ &\quad+\epsilon((1-\epsilon)x_{n-2}+\epsilon y_{n-3})))=\cdots. \end{aligned} \tag{13}$$

In general, $\eta\gg 1$ so that $0<\epsilon\ll 1$. Thus, to first order Eq. (13) becomes

$$y_n=(1-\epsilon)x_n+\epsilon x_{n-1}=(1-\epsilon)x_n+\epsilon F^{-1}(x_n), \tag{14}$$

where $F^{-1}(\ )$ is the inverse of the skew Ulam map. Due to the fact that each point x has two pre-images under the map, the attractor consists of two branches, as shown in Fig. 7(a). The distance between the two branches is proportional to ϵ. Figure 7(b) shows the first-order approximation of the reconstructed attractor from the filtered signal, or the return map. The second order approximation can be obtained similarly by omitting all the $O(\epsilon^3)$ terms,

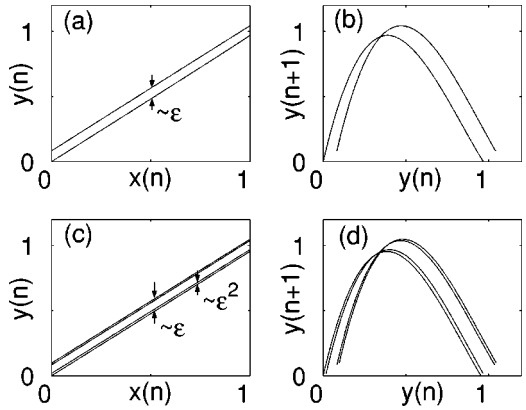

FIG. 7. The structure of filtered skew Ulam maps for $\epsilon=e^{-3}$. (a), (b) First-order approximations of the filtered attractor and the reconstructed attractor from the filtered signal y, respectively. (c), (d) The corresponding second-order approximations.

$$y_n=(1-\epsilon)x_n+\epsilon x_{n-1}-\epsilon^2 x_{n-1}+\epsilon^2 x_{n-2}, \tag{15}$$

where x_{n-2} can be obtained by iterating the inverse map two times from x_n. Consequently, the second-order attractor consists of four branches, as shown in Fig. 7(c). Each branch in the first-order attractor is now separated into two branches with the distance proportional to ϵ^2 in the second-order approximation.

The above-mentioned branch-doubling procedure thus introduces a self-similarity into the attractor, resulting in an increase of the fractal dimension, no matter how small ϵ is. Of course, when ϵ is very small, i.e., the cutoff frequency of the fitler is much larger than the bandwidth of the chaotic signal, the increment of fractal dimension is negligible. The above-mentioned observations are consistent with the result in Ref. 1.

For the filtered Ulam map, while the fractal dimension is increased under filtering, the topological entropy is invariant, because all branches of the filtered attractor can be mapped back to the original one-dimensional one-hump map. In principle, topological entropy can be computed provided that the critical point of each one-hump curve in the filtered return map can be located. For our model, this can be done by locating the set of all critical points, as shown in Fig. 8.

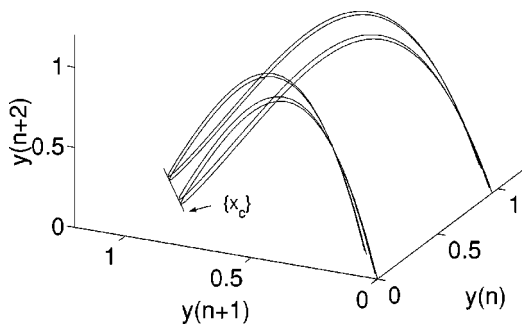

FIG. 8. The reconstructed attractor from filtered signal y in the three-dimensional space, where $\{x_c\}$, the set of critical points of all one-hump branches, is the generating partition.

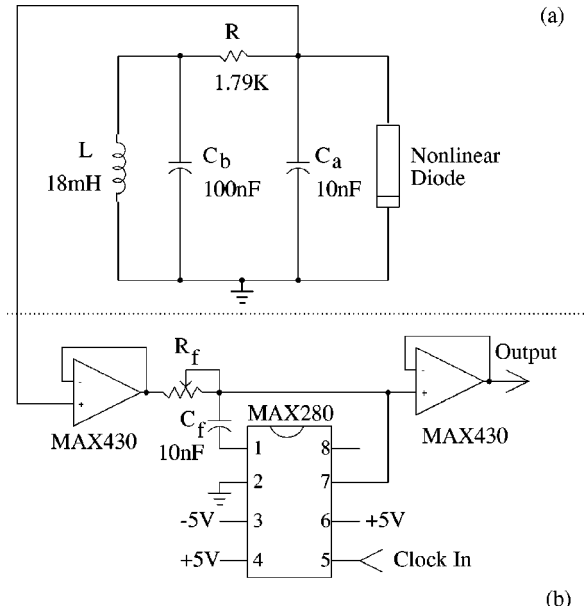

FIG. 9. Schematic diagram of the experimental circuit: (a) Chua's circuit, and (b) filtering circuit. In (b), two operational amplifiers (MAX430) are used as buffers, and R_f, C_f, and a third operational amplifier (MAX280) constitute a fifth-order Butterworth lowpass filter with cutoff frequency determined by the value of $\tau_f = R_f C_f$ and the frequency of an external clock.

Unfortunately, finding a generating partition for high-order filters and/or high-dimensional attractors is extremely difficult.

On the other hand, for an mth-order FIR filter given by

$$y_n = \sum_{i=0}^{m} a_i x_{n-i},$$

where a_i are the filter coefficients, there are exactly 2^m branches in the return map for one-hump maps, indicating that in theory, FIR filters do not increase the dimension of the return map. However, when we estimate the fractal dimension by using the measured signal filtered by a high-order FIR filter, the filtered map resembles the one filtered by an IIR filter and the computation can lead to an increase in the fractal dimension. The topological entropy is nevertheless invariant with respect to FIR filters, for the same reason as for IIR filters.

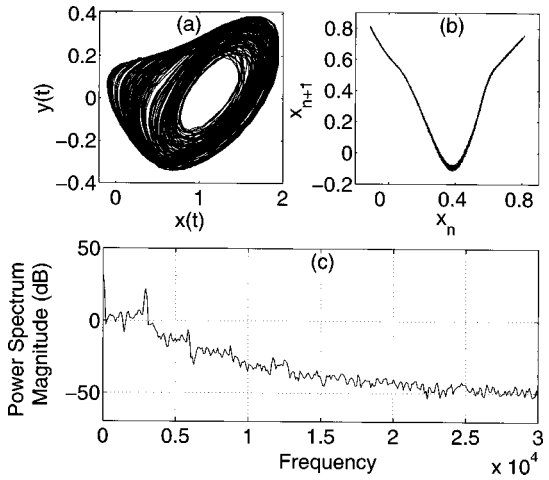

FIG. 10. (a) A single-scroll chaotic attractor from the experimental Chua's circuit projected on the (x,y) plane. (b) The return map constructed by recording the local minima x_n of time series $x(t)$. (c) Fourier power spectrum of $x(t)$. The bandwidth of $x(t)$ is about 2.5 kHz.

IV. EXPERIMENTAL VERIFICATION

We here provide experimental results that are consistent with the numerical and theoretical analysis in Secs. II and III. We utilize Chua's circuit, as shown in Fig. 9, where part (a) is the circuit itself with parameters set so that it generates a single scroll chaotic attractor and part (b) is a lowpass filtering circuit. The differential equations that describe the experimental Chua's circuit are

$$\begin{aligned} \frac{dx}{dt} &= \frac{1}{C_a}[G(y-x)-f(x)], \\ \frac{dy}{dt} &= \frac{1}{C_b}[G(x-y)+z], \\ \frac{dz}{dt} &= -\frac{1}{L}y. \end{aligned} \tag{16}$$

The signal $x(t)$, which is the voltage across the capacitor C_a, is fed into the filter (MAX280, MAXIM). The MAX280 chip is itself a fourth-order, switched capacitor filter, but when combined with the RC subcircuit consisting of R_f and C_f, it becomes a fifth-order all-pole lowpass filter with no DC error. The cutoff frequency of on-chip filter is set by an external clock (33120A, Agilent), with the clock-to-cutoff-frequency ratio of 100:1. The elements R_f and C_f also act as part of a feedback loop for the filter and contribute one pole in the complex-frequency response function of the filter. If the value of C_f is selected first, then the value of R_f is given by[29]

$$R_f = \frac{1.62}{2\pi C_f f_{\text{cut}}}, \tag{17}$$

where f_{cut} is the cutoff frequency defined at the -3 dB point of the frequency response function, which can be changed systematically in our experiments by varying the resistance R_f. The circuit is powered by a low-ripple and low-noise power supply (HPE3631, HP). The voltage signals are recorded by using a 12 bit data acquisition board (KPCI3110, Keithley) with sampling rate about 30 times the bandwidth of the signals.

Figure 10(a) shows, before filtering, projection on the (x,y) plane of the single-scroll chaotic attractor obtained for the set of parameter values specified in the circuit diagram (Fig. 9). The return map constructed from the local minima of the signal $x(t)$ is shown in Fig. 10(b). We notice a close resemblance between this experimental return map and the one from numerical simulation [Fig. 1(b)]. The power spectrum of $x(t)$ is shown in Fig. 10(c), where we see that the bandwidth of the signal, after subtracting off the -50 dB noisy background, is about 25 kHz. Figures 11(a)–11(d) show the return maps constructed from the filtered signals for the value of the cutoff frequency of $f_{\text{cut}} = 5$, 4, 3, and 2 kHz, respectively. We observe that these experimentally ob-

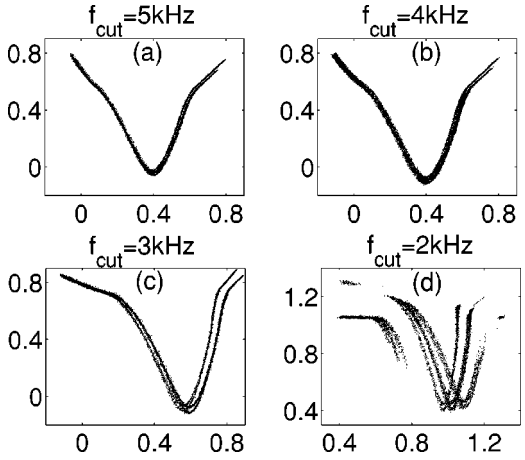

FIG. 11. From the experimental Chua's circuit, return maps obtained from the filtered signal of $x(t)$. (a)–(d) Cutoff frequency $f_{\text{cut}}=5$, 4, 3, and 2 kHz, respectively.

tained return maps are, to a high degree, consistent with the numerical ones [Figs. 2(a)–2(d)]. In particular, the single-branched structure of the return map is maintained when the cutoff frequency is not too low [Figs. 11(a) and 11(b)]. When the degree of filtering is severe (corresponding to lower value of f_{cut}), a multibranched structure in the return map arises. Thus, the behaviors of the topological-entropy-vs-f_{cut} function and BER-vs-f_{cut} function will be similar to that depicted in Figs. 3 and 5, although obtaining fine plots of these functions is beyond our reach at present due to the extremely stringent requirement of noise control and extremely long time data recordings in order for the fine structure of the function to be resolved.

Figures 12(a)–12(c) show the average first return time $\langle\tau\rangle$, the topological entropy, and the BER for four values of the cutoff frequency, respectively. For each fixed value of f_{cut}, we record the signal $x_f(t)$ after filtering, which contains at least 10^5 oscillations. The entropy is estimated by linear fitting to the plot of $\ln N(n)$ vs n, where n is up to 13. The BER is obtained by monitoring the fraction of symbols, out of 10^5, that are represented incorrectly with respect to the partition associated with the return map. In Fig. 12, the stars denote the entropies or BERs when no adjustment of the partition is made (i.e., the symbolic partition from the original, unfiltered signal is utilized), while the circles indicate the entropies or BERs when optimal partitions are chosen for the filtered signals, as described in Sec. II. We see that when the value of cutoff frequency is not too low, e.g., $f_{\text{cut}}>2.5$ kHz, both $\langle\tau\rangle$ and h_T with optimal partition are constant, indicating the invariance of the h_T of the chaotic flow. As discussed in Sec. II, at present, it appears difficult to assess whether h_T is invariant or not for severe filtering. We also see that for both high and low values of cutoff frequency, the improvement in BER is only incremental by choosing an optimal partition. The reason is, as we wish to reiterate here, that if the cutoff frequency is high, then the effect of filtering is minimal so that the partition estimated from the unfiltered signal is almost a generating partition for the filtered signal (in this case, the topological structure of the chaotic return map is hardly influenced by filtering). For

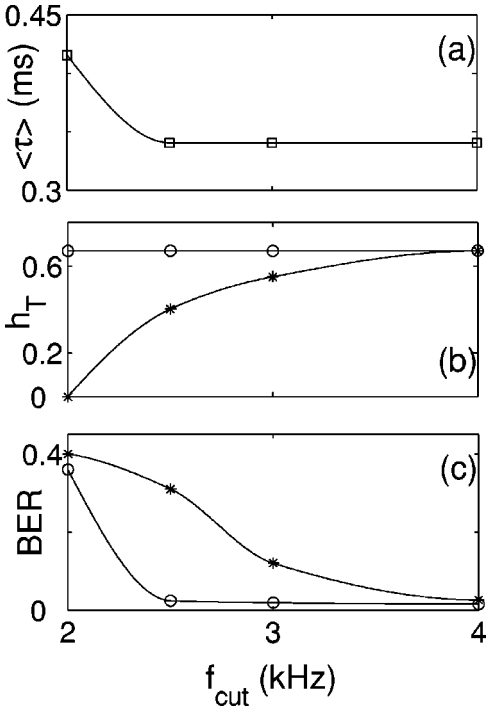

FIG. 12. From the experimental Chua's circuit. (a) The average first-return time $\langle\tau\rangle$ vs the cutoff frequency of the lowpass filter f_{cut}. (b) Topological entropy vs f_{cut}. (c) BER vs f_{cut}. The traces with circles are obtained with optimal partitions and the traces with stars are obtained with the generating partition P^{*0} of the unfiltered signal.

example, for $f_{\text{cut}}=4$ kHz, the BER from the original partition is about 2.6% and that from an optimal partition is about 1.5%, both are quite low. If, however, the cutoff frequency is very low, then the underlying dynamics for the filtered signal is essentially high-dimensional and the return map is multi-branched. In this case, no partition can yield significantly lower values of BER than any others. When the cutoff frequency is neither too large nor too small, we observe a significant improvement in BER when utilizing an optimal partition. For instance, for $f_{\text{cut}}=2.5$ kHz, the BER from the original partition is about 31%, but that from an optimal partition is about 2.4%—an improvement of more than one order of magnitude. The overall message is that if the effect of filtering is not too severe, then the reliability of the transmitted information can be guaranteed if the return map remains single-branched and an optimal symbolic partition is utilized.

V. DISCUSSIONS

In summary, our investigation of the effect of filtering on symbolic dynamics of chaotic signals indicates that, if the degree of filtering is not severe, the symbolic dynamics can be easily recovered in the sense that the value of the topological entropy is not reduced and the BER can be low. We give intuitive arguments suggesting the invariance of the topological entropy under filtering. We choose to study low-dimensional chaotic systems because they are feasible models that allow the issues concerning the symbolic dynamics to be addressed. Our results complement the existing ones on

the dimension aspect to give a relatively more complete picture for the effects of filtering on chaotic signals in general.

In a broad sense, our study is relevant to signal-processing problems in biomedical engineering. Consider, for example, the analysis of electroencephalogram (EEG) of a patient with epilepsy, obtained via electrodes attached to the scalp of the patient. The EEG signal comes from the electrical activities of networks of neurons inside the brain. Because of layers of physical barriers such as the scalp between the neurons and the electrodes, and because of the limitation of the recording instrument, the observed EEG signal can naturally be regarded as the filtered representation of the internal electrical activities of the neurons. The question is then, to what extent does the EEG carry the information that reflects the normal or abnormal neural activities of the brain? Similar questions also arise in engineering signal processing and in digital communication. We believe these are meaningful questions worthy of further exploration.

ACKNOWLEDGMENTS

L.Z. and F.H. are supported by DARPA under Grant No. MDA972-00-1-0027. Y.C.L. is sponsored by AFOSR under Grant No. F49620-98-1-0400 and by NSF under Grant No. PHY-9996454.

[1] R. Badii, G. Broggi, B. Derighetti, M. Ravani, S. Ciliberto, A. Politi, and M. A. Rubio, Phys. Rev. Lett. **60**, 979 (1988).

[2] P. Paoli, A. Politi, G. Broggi, M. Ravani, and R. Badii, Phys. Rev. Lett. **62**, 2429 (1989); A. Chennaoui, J. Lieber, and H. G. Schuster, J. Stat. Phys. **59**, 1311 (1990); F. Mitschke, Phys. Rev. A **41**, 1169 (1990); S. H. Isabelle, A. V. Oppenheim, and G. W. Wornell, in *ICASSP-92 Proceedings* 5(IV) (IEEE, Piscataway, NJ, 1992), Vol. 5(IV), pp. 133–136.

[3] J. L. Kaplan and J. A. Yorke, in *Functional Differential Equations and Approximations of Fixed Points*, Lecture Notes in Mathematics Vol. 730, edited by H.-O. Peitgen and H.-O. Walter (Springer, Berlin, 1979).

[4] J. Stark and M. E. Davis, IEE Digest **143**, 1 (1994); K. M. Campbell and M. E. Davis, Nonlinearity **9**, 801 (1996); B. Hunt, E. Ott, and J. A. Yorke, Phys. Rev. E **54**, 4819 (1996); M. E. Davis, Physica D **101**, 195 (1997).

[5] L. M. Perora and T. L. Carroll, Chaos **6**, 432 (1996); Int. J. Bifurcation Chaos Appl. Sci. Eng. **10**, 875 (2000).

[6] D. S. Broomhead, J. P. Huke, and M. R. Muldoon, J. R. Stat. Soc. Ser. B. Methodol. **54**, 373 (1992).

[7] L. M. Pecora, T. L. Carroll, and J. F. Heagy, Phys. Rev. E **52**, 3420 (1995).

[8] N. Rulkov, M. Sushchik, L. S. Tsimring, and H. D. I. Abarbanel, Phys. Rev. E **51**, 980 (1995); S. Schiff, P. So, T. Chang, R. E. Burke, and T. Sauer, *ibid.* **54**, 6708 (1996); L. Kocarev and U. Parlitz, Phys. Rev. Lett. **76**, 1816 (1996).

[9] The phenomenon of synchronous chaos was pointed out in: H. Fujisaka and T. Yamada, Prog. Theor. Phys. **69**, 32 (1983); V. S. Afraimovich, N. N. Verichev, and M. I. Rabinovich, Radiophys. Quantum Electron. **29**, 747 (1986). It was independently discovered and it was pointed out for the first time in the following paper that the phenomenon can have potential application in nonlinear digital communication: L. M. Pecora and T. L. Carroll, Phys. Rev. Lett. **64**, 821 (1990). Since then, synchronization in chaotic systems has become one of the most active research areas in nonlinear dynamics. See, for example, W. L. Ditto and K. Showalter, Chaos (Focus Issue on Control and Synchronization of Chaos) **7**, 509–687 (1997).

[10] S. Hayes, C. Grebogi, and E. Ott, Phys. Rev. Lett. **70**, 3031 (1993); S. Hayes, C. Grebogi, E. Ott, and A. Mark, *ibid.* **73**, 1781 (1994); E. Bollt and M. Dolnik, Phys. Rev. E **55**, 6404 (1997); E. Bollt, Y.-C. Lai, and C. Grebogi, Phys. Rev. Lett. **79**, 3787 (1997); E. Bollt and Y.-C. Lai, Phys. Rev. E **58**, 1724 (1998); Y.-C. Lai, E. Bollt, and C. Grebogi, Phys. Lett. A **255**, 75 (1999); Y.-C. Lai, Int. J. Bifurcation Chaos Appl. Sci. Eng. **10**, 787 (2000).

[11] M. S. Baptista, E. E. Macau, C. Grebogi, Y.-C. Lai, and E. Rosa, Phys. Rev. E **62**, 4835 (2000).

[12] C.-C. Chen and K. Yao, IEEE Commun. Lett. **4**, 37 (2000); M. Sushchik, N. Rulkov, L. Lason, L. Tsimring, H. Abarbanel, K. Yao, and A. Volkovskii, *ibid.* **4**, 128 (2000); C.-C. Chen and K. Yao, IEEE Trans. Circuits Syst., I: Fundam. Theory Appl. **47**, 1663 (2000).

[13] Symbolic dynamics can be a powerful tool for analyzing chaotic time series. See, for example, H. Herzel, W. Ebeling, and A. O. Schmitt, Phys. Rev. E **50**, 5061 (1994); J. Kurths, A. Voss, P. Saparin, and A. Witt, Chaos **5**, 88 (1995); A. Neiman, B. Shulgin, V. Anishchenko, W. Ebeling, L. Schimansky-Geier, and J. Freund, Phys. Rev. Lett. **76**, 4299 (1996); R. Engbert, C. Scheffczyk, R. Krampe, J. Kurths, and R. Kliegl, in *Nonlinear Time Series Analysis of Physiological Data*, edited by H. Kantz, J. Kurths, and G. Mayer-Kress (Springer, Heidelberg, 1998); M. Lehrman and A. B. Rechester, Phys. Rev. Lett. **78**, 1 (1997); K. Mischaikow, M. Mrozek, J. Reiss, and A. Szymczak, *ibid.* **82**, 1144 (1999); M. B. Kennel and A. I. Mees, Phys. Rev. E **61**, 2563 (2000); R. Steuer, W. Ebeling, D. F. Russell, S. Bahar, A. Neiman, and F. Moss, *ibid.* **64**, 061911 (2001); C. Bandt and B. Pompe, Phys. Rev. Lett. **88**, 174102 (2002).

[14] R. C. Adler, A. C. Konheim, and M. H. McAndrew, Trans. Am. Math. Soc. **114**, 309 (1965).

[15] The notion of *generating partition* (Ref. 30) is based on the ''splitting'' of the phase space in terms of measurable sets (Ref. 31). Consider an N-dimensional dynamical system, $\mathbf{x}_{n+1}=\mathbf{f}(\mathbf{x_n})$, on a metric space M, $\mathbf{f}$: $M\rightarrow M$. A *finite* collection of disjoint open sets, $\{B_k\}_{k=1}^K$, where $B_k\cap B_j=\varnothing$ $(k\neq j)$, is defined to be a topological partition if the union of their closures exactly covers M: $M=\cup_{k=1}^K\overline{B_k}$ (Ref. 32). Given an initial condition $\mathbf{x}_0$ and the topological partition $\{B_k\}_{k=1}^K$, the trajectory $\{\mathbf{x}_i\}_{i=-n}^n$ defines a sequence of visited partition elements: $\{B_{\mathbf{x}_i}\}_{i=-n}^n$, where $B_{\mathbf{x}_i}$ is the partition element B_k such that $\mathbf{x}_i\in B_k$. The set of intersection of the images and preimages of these elements $\cap_{i=-n}^n\mathbf{f}^{(-i)}(B_{\mathbf{x}_i})$ is in general open and nonempty. For a faithful symbolic representation of the dynamics, the limit $\cap_{n=0}^{\infty}\cap_{i=-n}^n\mathbf{f}^{(-i)}(B_{\mathbf{x}_i})$ must be a single point. Given a dynamical system $\mathbf{f}$: $\mathcal{M}\rightarrow\mathcal{M}$ on a measure space $(\mathcal{M},F,\mu)$, a finite partition $P=\{B_k\}_{k=1}^K$ is generating if the union of all images and preimages of P gives the set of all μ-measurable sets F. In other words, the ''natural'' tree of partitions: $\vee_{i=-\infty}^{\infty}\mathbf{f}^{(i)}(P)$, always generates some sub-σ-algebra, but if it gives the full σ-algebra of all measurable sets F, then P is called *generating* (Ref. 31). This weaker notion says that the splitting needs only be up to measurable sets.

[16] P. Grassberger and H. Kantz, Phys. Lett. A **113**, 235 (1985); P. Grassberger, H. Kantz, and U. Moenig, J. Phys. A **22**, 5217 (1989); P. Cvitanovic, G. Gunaratne, and I. Procaccia, Phys. Rev. A **38**, 1503 (1988); F. Giovannini and A. Politi, J. Phys. A **24**, 1837 (1991); F. Christiansen and A. Politi, Phys. Rev. E **51**, R3811 (1995); Nonlinearity **9**, 1623 (1996).

[17] R. Davidchack, Y.-C. Lai, E. M. Bollt, and M. Dhamala, Phys. Rev. E **61**, 1353 (2000).

[18] J. P. Eckmann and D. Ruelle, Rev. Mod. Phys. **57**, 617 (1985).

[19] Ja. B. Pesin, Sov. Math. Dokl. **17**, 196 (1976).

[20] A. Boyarsky and P. Gora, Trans. Am. Math. Soc. **323**, 39 (1991); N. Balmforth, E. Spiegel, and C. Tresser, Phys. Rev. Lett. **72**, 80 (1994).

[21] P. Collet, J. Crutchfield, and J. Eckmann, Commun. Math. Phys. **88**, 257 (1983); L. Block, J. Keesling, S. Li, and K. Peterson, J. Stat. Phys. **55**, 929 (1989).

[22] T. Matsumoto, IEEE Trans. Circuits Syst. **CAS-31**, 1055 (1984); R. Madan, *Chua's Circuit: A Paradigm for Chaos* (World Scientific, Singapore, 1993); L. O. Chua, C. W. Wu, A. Huang, and G.-Q. Zhong, IEEE Trans. Circuits Syst., I: Fundam. Theory Appl. **40**, 732 (1993); L. O. Chua, Int. J. Cir. Theory Applic. **22**, 279 (1994).

[23] E. N. Lorenz, J. Atmos. Sci. **20**, 130 (1963).

[24] O. E. Rössler, Phys. Lett. A **71**, 155 (1979).

[25] A. V. Oppenheim, A. S. Willsky, and S. H. Nawab, *Signals and Systems*, 2nd ed. (Prentice–Hall, Englewood Cliffs, 1997).

[26] E. M. Bollt, T. Stanford, Y.-C. Lai, and K. Życzkowski, Phys. Rev. Lett. **85**, 3524 (2000).

[27] E. M. Bollt, T. Stanford, Y.-C. Lai, and K. Życzkowski, Physica D **154**, 259 (2001).

[28] A. J. Lichtenberg and M. A. Lieberman, *Regular and Chaotic Dynamics*, 2nd ed. (Spring, New York, 1992).

[29] MAXIM Integrated Products, 1995.

[30] The concept of generating partition is often confused with the related ''Markov partition,'' whose existence implies that, in the case of an inter-

val map, end points of the partition map to end points (each partition interval is a homeomorphism onto a connected union of intervals from metric space *M*, i.e., intervals stretch exactly onto unions of intervals [P. Góra and A. Boyarsky, *Laws of Chaos, Invariant Measures and Dynamical Systems in One Dimension* (Birkhäuser, Boston, 1997)], and which can be appropriately defined for other classes of maps, such as axiom A [R. Bowen, Am. J. Math. **92**, 725 (1970); *Equilibrium States and the Ergodic Theory of Anosov Diffeomorphisms* (Springer, Berlin, 1975)].

[31] D. J. Rudolph, *Fundamentals of Measurable Dynamics, Ergodic Theory on Lebesgue Spaces* (Clarendon, Oxford, 1990).

[32] D. Lind and B. Marcus, *An Introduction to Symbolic Dynamics and Coding* (Cambridge University Press, New York, 1995).